Applicability of Solar Airflow Windows

Kelton Friedrich[a], Mohamed S. Hamed[a], Ghani Razaqpur[b], Simon Foo[c]
[a] *Thermal Processing Laboratory (TPL), Department of Mechanical Engineering, McMaster University, Hamilton, Ontario, Canada*
[b] *Department of Civil Engineering, McMaster University, Hamilton, Ontario, Canada*
[c] *Public Works and Government Services Canada, Ottawa, Ontario, Canada*

ABSTRACT

Accurate prediction of the performance of Solar Air Windows (SAWs) operating in various climates under real conditions has not been investigated. This paper reports the results of numerical simulations of SAWs carried out using ANSYS-CFX considering real boundary conditions. In order to determine the feasibility of SAWs, their performance has been examined in two similar office buildings located at two different climates. Each building has 30% of its south facing wall covered with SAWs in the spandrel areas. The results of the numerical simulations of the SAW operating in supply mode in January indicated that that for an office building located in Ottawa, Canada, 6% of its ventilation load and 12% of its heating load could be supplied by SAWs during a sunny day. Operating in exhaust mode in June, SAWs could be used to provide about 14% of the ventilation load of the office building located in Dubai, UAE.

1. INTRODUCTION

With the drive to reduce the use of non renewable resources, primarily derived from fossil fuels, achieving Net-Zero Energy Buildings (NZEB) has become the goal of building design. Solar airflow windows (SAWs), which can provide natural ventilation of conditioned air, is a promising technology that could help in achieving NZEB.

A SAW is a thermosyphon similar to the more well known concepts of Trombe Walls and solar chimneys. In its simplest form, a SAW is a cavity made of two vertical parallel plates. One plate is made of a glazing material that transmits solar radiation, allowing the radiation to be incident on the second parallel plate, which heats up as it absorbs the radiation. Consequently, the air next to the absorbing plate is heated. This heated air then rises, as hotter air is less dense relative to colder air. This mechanism induces a thermally driven flow between the two parallel plates.

Although there are four modes, SAWs operating in the supply and exhaust mode are the only ones considered in this paper. The exhaust mode is when the air enters the bottom of the cavity from the inside and exits the top to the outside, removing air from the building, providing natural ventilation. The supply mode occurs when air enters the bottom from the outside, and exits the top into the building, again providing natural ventilation and in addition can heat the building.

The past research directly related to SAWs has been on Trombe Walls and solar chimneys. The common approach is to have two parallel walls held at a constant temperature or heat flux as seen in the works such as Ayinde et al. (2006). The next approach is to have one parallel plate held at constant temperature or heat flux while the other is treated as adiabatic as seen in the the works of Chen et al. (2003), Zamora and Kaiser (2009). The real world case however is not like this. The glazing that allows the radiation through to heat up the absorbing wall is never perfectly transparent or perfectly insulated. Some experiments that allowed for this are La Pica et al. (1993), Hernandez et al. (2006), Burek and Habeb (2007). These experiments are the most likely to predict the performance of SAWs, as they include the most realistic boundary conditions.

The glazing surface transmits, reflects, absorbs, and emits radiation, along with conducting heat. These factors control the heat transfer into the cavity and can affect the flow patterns in the cavity. Since these heat transfer mechanisms have not been accounted for in pervious numerical research, improvements can be made to advance the predictive capabilities of numerical models of SAWs.

The main objective of this work is to investigate the performance of SAWs under real boundary conditions.

2. CONJUGATE PROBLEM

The current configuration modeled can be seen in Figure 1. There is an S-shaped channel and a glazing sheet with the absorbing wall opposite of it. The side that inlet and exit are situated on depends on the mode of the SAW.

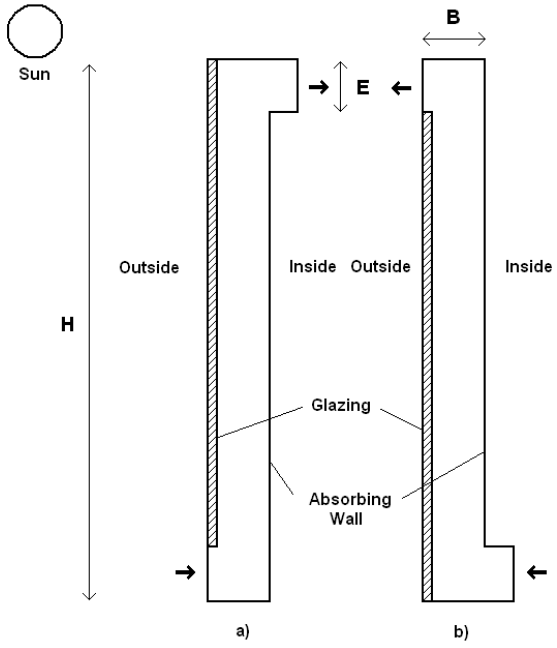

Figure 1. SAW Configuration for a) Ottawa Case Study (Supply mode) and b) Dubai Case Study (Exhaust mode). Dimensions used in current simulations H = 1.0 m, B = 0.1 m, E = 0.1 m

3. DETAILS OF THE PRESENT MODEL

Mathematical Formulation and Numerical Model

The simplified time-averaged Navier-Stokes equations of fluid flow can be written as follows:

$$\frac{\partial U_i}{\partial x_i} = 0, \quad (1)$$

$$U_j \frac{\partial U_i}{\partial x_j} = \frac{\partial}{\partial x_j}\left(\mu \frac{\partial U_i}{\partial x_j} - \rho\overline{u_i u_j}\right) - \frac{\partial p}{\partial x_i} + g_i \beta (T - T_\infty), \quad (2)$$

$$C_p \rho U_j \frac{\partial T}{\partial x_j} = \frac{\partial}{\partial x_i}\left(\lambda \frac{\partial T}{\partial x_j} - C_p \rho \overline{u_i T'}\right) \quad (3)$$

The commercial CFD software package of ANASYS-CFX version 12 was chosen as the numerical code. All the turbulence modeling was done with the Shear Stress Transport(SST) model of Menter (1994). All simulations in this paper were modeled as turbulent.

Validation

To validate if the current ANSYS CFX model used was capable of accurately simulating this problem, the ANSYS-CFX model was validated against a benchmark experiment. The experimental work of Chen et al. (2003) models a parallel plate cavity with one wall having uniform heat flux, the other insulated, the configuration can be seen in Figure 2. The Boussinesq approximation was used. The inlet and outlet were set as openings at the same constant pressure. This allows for swirling flow if it developed.

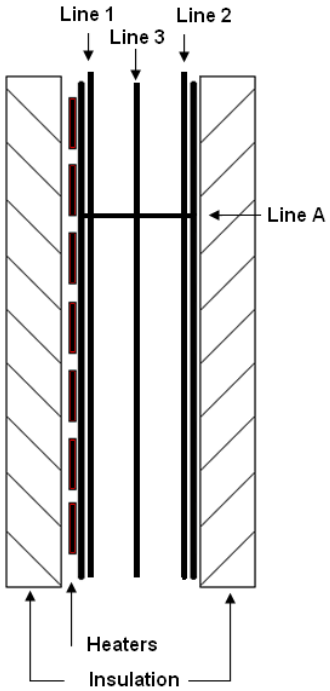

Figure 2. Two Dimensional view of Chen et al. (2003) set up. Line 1 - heated wall, Line 2 - non-heated wall, Line 3 - 12 cm away from heated wall, Line A - Horizontal line

The discrete radiation transfer model in ANSYS-CFX was only used for the numerical modeling of this experiment, and has not been used in any other simulations in this paper. Since the emissivity of the surfaces were not known they had to be estimated. The following plots show the numerical results plotted against the experimental. From Figure 3, it can be seen that the temperature of the walls is accurately predicted. However, the temperature in the flow field is under predicted by the numerical results. This is likely due to radiation heating the temperature probes in the experiment.

The numerical and experimental temperature results are plotted in Figure 4 in the vertical direction. The numerical predicts the temperature on the heated and non-heated walls relatively accurately. The numerical non-heated wall temperature can be matched almost exactly to the experimental results by adjusting the emissivity's of the surfaces.

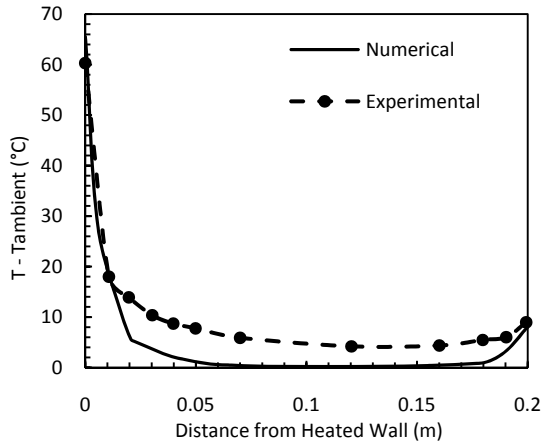

Figure 3. Temperature difference across parallel plate gap at line A, 1430 mm from inlet

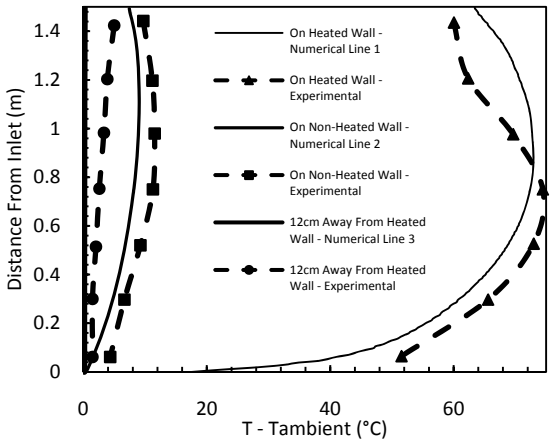

Figure 4. Vertical temperature difference along channel height at different locations

The velocity profile seen in Figure 5 gives the greatest confidence in the numerical model as the numerical and experimental agree. Due to the limitation of experiment, the near wall velocity could not be found so it is not possible to conclude that the numerical model predicted the near wall velocity correctly.

Even without accounting for the minor discrepancies, the numerical ANASYS-CFX model predicted the experimental results provided that the emissivity's used for the surfaces are correct. Given this level of accuracy of predicting the performance of simple thermosyphon configurations, there is a high level of confidence that the current numerical model can be used accurately on more complex configurations.

To further validate the current model, simulations were run to predict the previously published numerical work on Trombe Wall channels. If the current model gives the same results as a previous model, this will indicate that the current model is at the same state of the art as the current standard. For this reason a recent numerical study on turbulent flow in a cavity was chosen. The paper by Zamora and Kaiser (2009) investigated finding the optimal spacing between the vertical plates for an L shaped channel for different Rayleigh numbers ranging from laminar to turbulent. The case considered for comparison was a uniform wall temperature symmetrically heated channel with the same ambient temperature at the inlet and outlet. Three different turbulent Rayleigh number cases were considered, however only the results of one is presented. The vertical plate spacing to height and entrance height to height ratios were both set to 0.1. From the comparison of the results in Table 1, it can be seen that the current model does follow the predictions of the previous work by Zamora and Kaiser (2009).

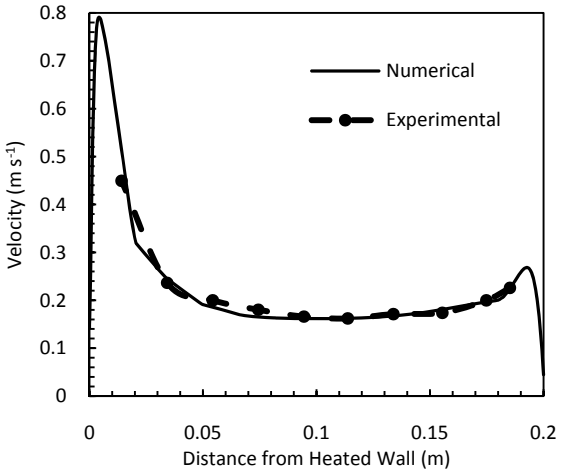

Figure 5 Velocity across gap, 1100 mm above the inlet

Table 1. Comparison of current model results with Zamora and Kaiser (2009)

CASE	DIMENSIONLESS MASS FLOW	NUSSELT # ON WALL OPPOSITE INLET	NUSSELT # ON WALL ABOVE INLET	Y^+
RA = $5x10^{10}$				
ZAMORA & KAISER	4420	338	274	.8
PRESENT STUDY	4408	307	317	0.78
DIFFERENCE	0.2%	9.2%	15.7%	

One can expect there to be different results as different turbulence models were used, as well as different numerical solvers, explaining why there is a difference in the results. So given that the present model predicted similar results for the same case as previous models, it can be concluded that the current model is capable of the current standard, and can be used on more complex configurations with relative certainty.

The numerical ANSYS model was validated, and having confidence that the simpler problems can be predicted accurately, the model was expanded to model more real world boundary conditions.

Setup of Numerical Code

For each different level of heat flux, a steady state simulation was done to estimate the results for that range. The flow was considered incompressible given the low velocities. The fluid considered was air at 25°C. The Boussinesq approximation was used. The SST model was used due to its ability to predict the flow patterns in the benchmarking of simpler problems. The inlet turbulence intensity was set to 5%.

A non uniform, unstructured grid was used for all simulations. It was concluded that a grid containing 60,000 nodes, with a rough spacing of 78 X 570 cells in the main cavity, gave results that are no longer dependant on the grid. The convergence criterion was set to having the normalized residuum (RMS) below 1.0e-04.

Boundary Conditions

The energy source to drive the SAWs is the radiation from the sun. This energy source is very transient, changing throughout the day as the earth rotates about its axis, as well as throughout the year throughout the earth's orbit. To reduce the need for a yearlong transient simulation, a reprehensive day is selected in the season the SAW will be operating in, and the day is broken in to qusi-steady time intervals of one hour. So at each time interval the average heat flux for that hour is used to find the linear interpolated performance of the SAW from the simulations run at steady state. The determination of the heat flux at every hour was done following the ASHRAE solar model in the ASHRAE Fundamentals handbook (2009).

The boundary conditions were set up in the following manner to account for the conjugate problem. There was a glass and fluid domain. The outside glass surface was set with a heat transfer coefficient and a outside temperature. The temperature on the outside is set based on the case study being considered. The outside opening and inside opening were set to their respective temperatures. The rest of the walls were set to adiabatic Q = 0, assuming the heat transfer through them is negligible. Outside and inside openings were set to allow flow into or out of the cavity based on pressure P = 0, and both openings where set at the same reference pressure. All walls were set with the no slip condition for solving the momentum equation, u=v= 0. The sides where set with the symmetry condition to allow of simulation of a two dimensional flow, $\frac{\partial U_i}{\partial x_i} = 0$. The source terms included having 10% of the incident radiation heat flux being absorbed uniformly throughout the glass material. The heat flux on the absorbing back wall was assumed to be 75% of the incident radiation heat flux, this gives a total of 85% of the incident heat flux being absorbed by the system with 15% being reflected or emitted back out.

A double glazed window was selected as this is the industry standard for exterior glazing due to its low thermal conductivity to cost ratio. The effective thermal conductivity used was 0.0235 W m^{-1} K^{-1}. The window thickness was 0.015 m, and the external convection coefficient was 5 W m^{-2} K^{-1}. The temperature boundary conditions for the outside where chosen based on the average weather data for the month considered. The inside was assumed to be 21^{o} C as this is the standard comfort setting. The top, bottom and absorbing wall side of the apparatus was assumed to be adiabatic to simplify the problem. A one meter tall S-shaped channel was selected. The gap to height and spacing to height ratio of 0.1 came from pervious numerical work on the optimized spacing for mass flow rate of Zamora and Kaiser (2009).

4. Results and Discussion of Numerical Simulation

Given the above inputs, steady state simulations were run for various incremental heat fluxes on the absorbing wall. Figure 6 and 7 show the streamlines and temperature contours for both cooling and heating mode for a single constant heat flux of 400 W on the absorbing wall. The Dubai case has a higher flow rate, and there is little to no recirculation at the inlet, where as the low flow rate of the Ottawa case leads to recirculation at the inlet. In both the Dubai and Ottawa case, there is recirculation at the exit, with the heated exiting air leaving at the top of the exit. For the Ottawa case the air falls along on the cold glass, making a large recirculation zone throughout the cavity. In the Dubai case the air rises on both sides of the cavity, but due to the recirculation at the exit, air heated on the glass side has to cross to the absorbing wall side. The temperature contour in the Dubai case does change fast throughout the cavity because there is not much temperature change from the inlet to outlet, and the large temperature change happens right next to the absorbing wall, and stays along the top of the cavity with the hot air. Since there is a large change in temperature from the inlet to the exit in the Ottawa

case there is a change in air temperature throughout the cavity.

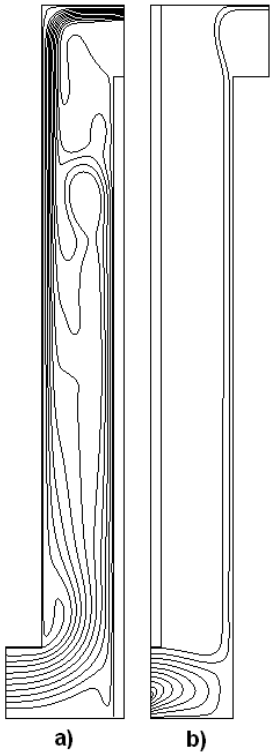

Figure 6. Streamlines of a) Dubai cooling mode b) Ottawa heating mode

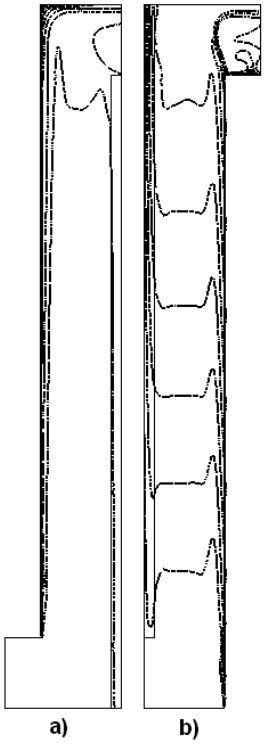

Figure 7. Temperature contour of a) Dubai cooling mode b) Ottawa heating mode

At both the absorbing wall and in the glass, there is a high temperature gradient in both cases.

The volume flow rate is presented in the volume flow rate per unit width and can be seen in Figure 8. As one can see the flow rate increase with heat flux, which corresponds to when the sun is closer to the noon position.

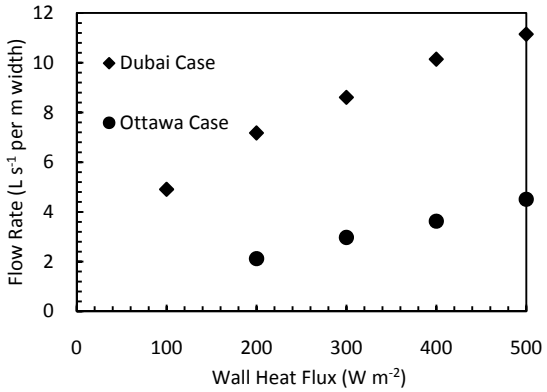

Figure 8. Volume flow rate per unit width as a function of the heat flux imposed on the absorbing wall

Comparing the Ottawa case study results to the Dubai case study, we can see that the mass flow rate is considerably smaller in the Ottawa case study for the same heat flux. This is due to the colder outside temperature relative to the inside temperature. The colder outside temperature increases the heat loss through the glazing reducing the amount of energy available to drive the system. Also the cold air takes more energy to heat up, and for the SAW to provide ventilation, the air inside the SAW must become warmer than the inside air. So since the temperature difference between the inside and outside air is greater in the Ottawa case than the Dubai case, the solar radiation has to heat the air inside the SAW to a higher a temperature difference with respect to the exit air temperature, to get a large enough pressure differential to drive the flow.

The average exit temperature is shown in Figure 9, with the temperature increases with increasing heat flux. What is interesting to note is that the Ottawa case has to heat up the air 31°C more than the Dubai case.

5. CASE STUDIES

To give an indication of what the numerical results mean in a real world situation, the results were applied to the same building located at Ottawa and Dubai. The difference between the locations is the climate and the season. A 45 m square floor plan by 25 stories was assumed, with a capacity for 5000

people. If there is three meters per story, and no shading on the building, there is 3,375 m^2 of south facing area exposed to the sun. Based on ASHRAE Standard 62.1 (2007), 20 CFM (10 L/s) per person is required in an office building to maintain the current standard of air quality. This gives a ventilation load of 50,000 L/s during occupied hours for both case studies. The one meter high SAW would be placed in the spandrel areas, and given that the stories are three meters high, the one meter high SAWs will cover 30% of the south facing area.

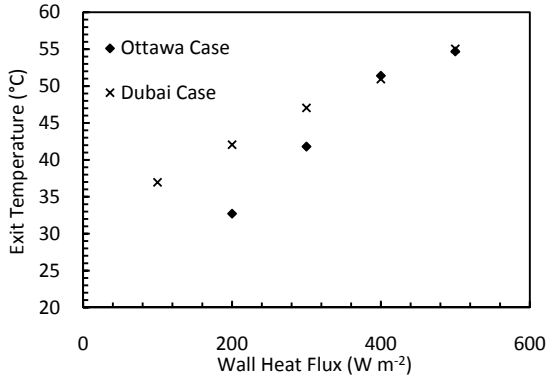

Figure 9. Mass flow averaged Exit temperature

Ottawa Case Study

Having a SAW operating in supply mode in the winter time is the most advantageous set up, as this provides fresh air as well as pre heating the fresh air, offsetting both the mechanical fan and heating requirements. A day in January was selected to be the representative day for this case study. Reported by ASHRAE (2009) the average temperature for Ottawa is -10^o C in January. Assuming little to no humidity, the energy requirement to heat the 50, 000 L s^{-1} of outside air to 21^o C is 1.822 MW. With 30% of the south facing area being used and an average heat flux of 443 W m^{-2} for a 7.5 hour period, meaning there is a max potential of offsetting 0.449 MW or 25% of the thermal ventilation load.

Using the results from the numerical simulation and using a linear line that fits the data points well, one can interpolate the mass flow rate for the various hours of the day as seen in Figure 10. Averaging these values to get a daily average flow rate per unit depth, multiplying this value by the 30% of the area used to get the total average flow rate, which is 3,206 L s^{-1} or 6.4% of the ventilation load. The same process can be done with the temperature increase to find the daily average temperature increase. Multiplying the temperature increase by the mass flow rate to find the amount of thermal load that is offset by the SAW gives 0.217 MJ or 12%.

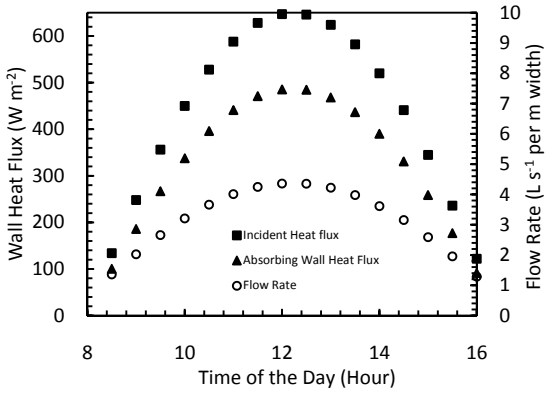

Figure 10. Ottawa Case ASHRAE solar model predicted incident heat flux on window, 75% becoming the heat flux on the absorbing wall which is used to find the flow rate from the current model of the SAW

Dubai Case Study

Having a SAW operation in exhaust mode in the summer time is a useful set up, as this removes stale air from inside the building, offsetting the mechanical fan requirements. However since the air drawn in would be at the ambient temperature, which is above the desired air temperature and since SAW's only heat air, there would be no reduction in the thermal cooling load. A day in June was selected to be the representative day for this case study. Reported by ASHRAE (2009) the average temperature for Dubai is 35^o C in June.

As was done with the pervious case study, the results from the numerical simulation can be used to interpolate the mass flow rate for the various hours of the day as seen in Figure 11. Averaging these values to get a daily average flow rate per meter depth, multiplying this value by the 30% of the area used to get the total average flow rate, which is 7,033 L s^{-1} or 14% of the ventilation load.

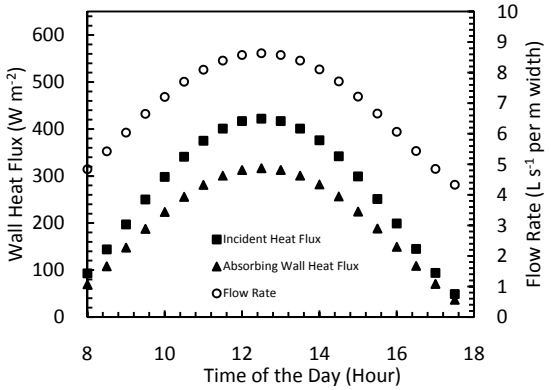

Figure 11. Dubai Case ASHRAE solar model predicted incident heat flux on window, 75% becoming the heat flux

on the absorbing wall which is used to find the flow rate from the current model of the SAW

When comparing the two case studies, one can see that the solar intensity for the Ottawa case is higher, this is due to the vertical window being closer to being perpendicular to the sun during the winter. However the Dubai case has more hours of sun, as the days are longer in the summer.

6. Conclusions and Future work

Seen by the case studies, there is the potential for SAW to reduce the thermal and ventilation loads of mechanical HVAC systems in buildings. The numerical simulations to derive these predictions for SAWs have more boundary conditions that simulate the real world conditions of any numerical work done previously. Hence the predictions of the present numerical work should be the closet to real case so far. However, even though more complex boundary conditions were used, many of them were arbitrarily picked and may not be the correct assumptions to model the real case. Also the SAW numerically modeled where not necessarily optimized for the conditions they were placed in. So there is still much work to be done to improve the performance of the systems.

To validate the current numerical model on the more complex problem, experimental work will need to be preformed. A few experimental trials will provide enough information to validate the current numerical model and also provide values to replace the arbitrarily picked boundary conditions in the current model. Once validated and with improved boundary conditions the numerical model can be used to simulate a variety of SAW configurations. This will allow for a parametric study to find the optimal geometric and material properties for giving the most mass flow or thermal efficiency. With an energy simulation program, the daily, seasonal or year round averaged optimal properties could be determined. Knowing the expected performance at the optimal system, feasibility studies can be preformed to find out the expected payback period of SAW, so that it can be compared to other green technologies.

Acknowledgement

The authors would like to acknowledge the financial support received from Public Works and Government Services Canada.

References

ASHRAE. 2007. Standard 62.1 - 2007: Ventilation for Acceptable Indoor Air Quality. American Society of Heating, Refrigerating and Air-conditioning Engineers Inc.

---. 2009. *2009 ASHRAE Handbook - Fundamentals*. Atlanta, GA: American Society of Heating, Refrigerating and Air-conditioning Engineers Inc.

Ayinde, T. F., S. A. M. Said & M. A. Habib (2006) Experimental investigation of turbulent natural convection flow in a channel. *Heat and Mass Transfer,* 42**,** 169-177.

Burek, S. A. M. & A. Habeb (2007) Air flow and thermal efficiency characteristics in solar chimneys and Trombe Walls. *Energy and Buildings,* 39**,** 128-135.

Chen, Z. D., P. Bandopadhayay, J. Halldorsson, C. Byrjalsen, P. Heiselberg & Y. Li (2003) An experimental investigation of a solar chimney model with uniform wall heat flux. *Building and Environment,* 38**,** 893-906.

Hernandez, V., D. Morillon, R. Best, J. Fernandez, R. Almanza & N. Chargoy (2006) Experimental and numerical model of wall like solar heat discharge passive system. *Applied Thermal Engineering,* 26**,** 2464-2469.

Lapica, A., G. Rodono & R. Volpes (1993) AN EXPERIMENTAL INVESTIGATION ON NATURAL-CONVECTION OF AIR IN A VERTICAL CHANNEL. *International Journal of Heat and Mass Transfer,* 36**,** 611-616.

Menter, F. R. (1994) 2-EQUATION EDDY-VISCOSITY TURBULENCE MODELS FOR ENGINEERING APPLICATIONS. *Aiaa Journal,* 32**,** 1598-1605.

Zamora, B. & A. S. Kaiser (2009) Optimum wall-to-wall spacing in solar chimney shaped channels in natural convection by numerical investigation. *Applied Thermal Engineering,* 29**,** 762-769.